First-principles investigations of disorder effects on electronic structure and magnetic properties in Sr_2CrMoO_6

2008 J. Phys.: Condens. Matter 20 255230

(http://iopscience.iop.org/0953-8984/20/25/255230)

J. Phys.: Condens. Matter **20** (2008) 255230 (8pp) doi:10.1088/0953-8984/20/25/255230

First-principles investigations of disorder effects on electronic structure and magnetic properties in Sr_2CrMoO_6

Q F Li[1,2], X F Zhu[2] and L F Chen[2]

[1] Department of Physics, Nanjing University of Information Science and Technology, Nanjing 210044, People's Republic of China
[2] Department of Physics, Nanjing Normal University, Nanjing 210097, People's Republic of China

E-mail: smileqfli@163.com

Received 11 December 2007, in final form 7 May 2008
Published 22 May 2008
Online at stacks.iop.org/JPhysCM/20/255230

Abstract

The electronic structures and magnetic properties are reported for ordered and disordered Sr_2CrMoO_6 presenting oxygen vacancies or/and antisite defects (ASs). We investigate the stability of an antiparallel (AP) magnetic moment on Cr antisites and the calculations show that these solutions are more stable relative to the parallel solution for AS defects with or without oxygen vacancies. Electronic band structure calculations indicate that the perfect Sr_2CrMoO_6 is half-metallic, and the half-metallic character is preserved for Sr_2CrMoO_6 containing only oxygen vacancies, while the half-metallic nature is destroyed when 25% ASs (50% ASs) with or without oxygen vacancies is present. For 25% ASs with two oxygen vacancies, the system possibly shows nonmetallic behavior. The experimentally observed reduction of the magnetic moment mainly arises from an antiferromagnetic coupling of Cr–O–Cr (Cr–Cr) bonds in a disordered sample.

(Some figures in this article are in colour only in the electronic version)

1. Introduction

Double-perovskite oxides have attracted a great deal of attention [1–5] owing to their potential applications in magnetotransport devices as well as their rich and challenging physical properties. Some compounds [6–8] of the type $A_2BB'O_6$ tend to adopt the perovskite structure, where A can be an alkali-earth element such as strontium, calcium, or barium or a lanthanide, and B and B′ are different transition metals. Each transition-metal site is surrounded by an oxygen octahedron sometimes heavily distorted, and the A atoms are situated in the holes produced by eight adjacent oxygen octahedra. A large difference in charge or size between B and B′ can lead to their ordered arrangement in the perovskite lattice.

Up to the present, the structural and magnetic properties of Sr_2CrMoO_6 have been widely studied in experiment for the high T_N [9] and particular nonmetallic behavior [10, 11]. In the idealized ordered Sr_2CrMoO_6 each of the two transition-metal sites, namely, the Cr^{3+} ($3d^3$) and Mo^{5+} ($4d^1$) sites, is believed to be ferromagnetically arranged within each sublattice, while the two sublattices are supposed to be coupled antiferromagnetically, giving rise to an $S = 1$ state. Recently, it has been found that it is possible to synthesize samples of Sr_2CrMoO_6 with oxygen vacancies [12] as well as substantial mis-site disorders where Cr and Mo sites interchange their positions [9, 10, 12]. Such a disorder is found to have profound effects on the physical properties of this compound [11, 13, 15], particularly in terms of its magnetic and electronic properties. Moritomo *et al* [11] have found that Sr_2CrMoO_6 is ferrimagnetic with a low magnetic saturation 0.5 μ_B at 5 K and has a semiconducting behavior. In addition, Arulraj *et al* [13] have reported a ferrimagnetic transition at 450 K for Sr_2CrMoO_6. These authors found a magnetic moment much smaller than the expected one (2.0 μ_B per formula unit (f.u.)). Due to the similar ionic sizes [14] of Mo^{5+} and Cr^{3+} (0.61 and 0.615 Å, respectively), there is considerable site disorder. From the

Rietveld refinement of the x-ray data [15], the percentage order in the Sr_2CrMoO_6 is found to be 65%. X-ray diffraction (XRD) measurements find that Cr (Mo) disorder is 43% [10]. In an early report [9], 50% ordering was reported. At the same time, the x-ray refinements [12] detect the presence of oxygen vacancies, and the concentration of vacancies can be very high. The concentration of oxygen vacancies is 8.83% at T_N. Therefore, a relationship between oxygen vacancies and cation disorder cannot be discarded. Nevertheless, this magnetization reduction and the semiconducting behavior are never calculated for both types of imperfections (oxygen vacancies and antisite defect), and the band structure has been reported [16, 17] only for Sr_2CrMoO_6 with a perfect structure. It is well known that synthesized samples present a reduced magnetic moment that strongly depends on the synthesis process, purity and antisite (AS) displacement. However, the microscopic origin of the reduction in the saturation magnetic moment is still not entirely clear. Do the oxygen vacancies or/and antisite defects affect the magnetic properties and the half-metallic character of perfect Sr_2CrMoO_6? What causes the magnetization reduction and the particular nonmetallic behavior? All of these problems are interesting. Detailed knowledge about the disordered compounds is therefore important for better understanding of the various experimental results and designing of samples with better magnetic and magnetoresistive properties. In this context, our work analyzes the importance of the oxygen vacancies and antisite (AS) defect perturbation from the point of view of the magnetization reduction and of the half-metallic character. In the following section, we briefly summarize the computational details. In section 3, we discuss the geometrical structures, magnetic moments and electronic structures of perfect Sr_2CrMoO_6 and disordered Sr_2CrMoO_6 with oxygen vacancies or/and antisite defects. Finally, we summarize our conclusions in section 4.

2. Computational details

The first-principles calculations in this paper are performed in a plane-wave basis set using the projector augmented wave (PAW) [18, 19] method in the generalized gradient approximation (GGA) as it is implemented in the VASP [20, 21] program. We also have employed the DFT + U methodology [22–25] which is able to significantly improve predictions of phase stability and thermodynamic properties as well as magnetic and electronic structure in oxides. We use here the simple formulation by Liechtenstein, Anisimov, and Zaanen [24] and Dudarev *et al* [25], where a single parameter U_{eff} determines an orbital-dependent correction to the DFT energy. U_{eff} is generally expressed as the difference between two parameters, the Hubbard U, which is the Coulomb-energetic cost to place two electrons at the same site, and an approximation of the Stoner exchange parameter J, which is almost constant at 1 eV [26]. The DFT + U correction acts by reducing the one-electron potential locally for the specified orbitals of the metal atoms, therefore reducing the hybridization with the ligands.

In order to compare the magnetic properties and electric structures of the ordered and the disordered Sr_2CrMoO_6, calculations were performed by constructing supercells of four formula units for Sr_2CrMoO_6 with or without ASs, and larger supercells were constructed for Sr_2CrMoO_6 presenting oxygen vacancies with or without ASs. The number of plane waves is controlled by the cut-off energy, which in all our static calculations was $E_{\text{cut}} = 400$ eV, while all the geometry relaxations were performed with an increased cut-off of 520 eV to ensure proper convergence of the stress tensor. The atomic geometries are fully optimized by the Hellmann–Feynman forces on atoms and stressed on the supercell. The relaxations of lattices are stopped until the forces on each ion are converged to less than 0.01 eV $Å^{-1}$. For the Brillouin zone integration, the tetrahedron method is used for the final total energy calculations with optimized crystal structures. For sampling the irreducible wedge of the Brillouin zone, we use a denser k-point grid for final total energy calculation than for geometry optimization. To explore the effects of the on-site Coulomb energy U on the electronic structures and the magnetic moments, specific values for Cr ($U = 3.0$ eV [27]and $J = 0.87$ eV [22]) are used in the GGA + U calculation.

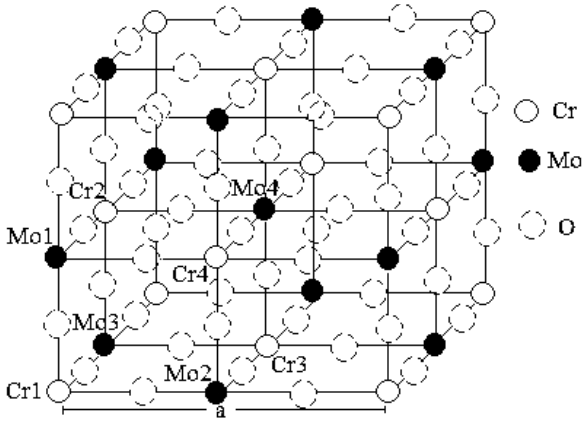

Figure 1. Crystal structure of the perfect double perovskite Sr_2CrMoO_6.

3. Results and discussion

3.1. Magnetic properties and electronic structure of perfect Sr_2CrMoO_6

For the perfect Sr_2CrMoO_6 case, the calculated crystalline structure is cubic with lattice parameter $a = 7.865$ Å as shown in figure 1. The result is slightly larger than the experimental value [28, 12]. The calculated magnetic moments of B and B′ sites are listed in table 1 using GGA and GGA + U methods. Obviously, taking the on-site Coulomb energy U into account (GGA + U), the spin moments of all the transition-metal atoms are, as expected, enhanced due to charge localization and enhanced exchange integral. Our calculations show that both the magnetic moments are suppressed as compared with the ideal values (3.0 μ_B and −1.0 μ_B for the Cr^{3+} and Mo^{5+} ions, respectively). Because of the diffusive 5s valence configuration and the ionic behavior of the alkaline-earth-metal element, the local moments of Sr ions are negligibly small. The spin moments on the oxygen ions are also small due to the nearly closed 2p shells, while the magnetic moments at B(Cr) site are

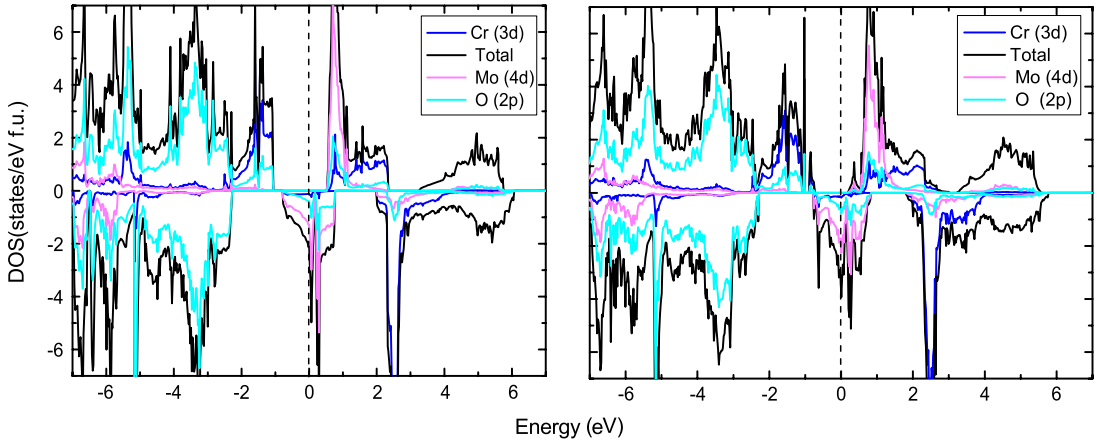

Figure 2. Total and partial densities of states of perfect Sr_2CrMoO_6 (left panel) and Sr_2CrMoO_6 with two oxygen vacancies (right panel) from GGA + U calculations. The spin-up and/or spin-down DOS is shown above and/or below the abscissa axis. The Fermi level is at zero energy.

Table 1. Calculated magnetic information for perfect Sr_2CrMoO_6. Experimental measurements are listed for comparison.

Magnetic moment	GGA	GGA + U	Expt.
μ_{B-site} (μ_B)	2.285	2.882	0.8[a]
$\mu_{B'-site}$ (μ_B)	−0.435	−0.636	—
μ_T (μ_B/f.u.)	2.0	2.0	0.5[b]

[a] Reference [12].
[b] Reference [11].

enhanced as compared with the experiment [12]. This may be related to the oxygen vacancies and antisite (AS) defects. We will discuss the effect in the following calculations of oxygen vacancies and AS defects. Note that the magnetic moments of Cr are aligned ferromagnetically and the moments on Mo are coupled antiferromagnetically to the Cr moments. Actually, Mo magnetic moments (i.e. antiparallel to the Cr moments) are induced by the hybridization of Cr 3d $t_{2g\downarrow}$ and Mo 4d $t_{2g\downarrow}$ states. In this sense, we regard the system as ferromagnetic. The calculated net magnetic moment (2.0 μ_B) is much larger than the experiment [12], which also correlates with the defect behavior as detailed below.

Figure 2 shows the calculated total density of states (DOS) and various partial densities of states from the spin-polarized GGA + U method. The calculations for the perfect structures give the ground state to be of half-metallic character with a finite density of states in the spin-down channel and a zero density of states in the spin-up channel near E_F and antiferromagnetic ordering between the high-spin $3d^3$ Cr^{3+} ion and the $4d^1$ Mo^{5+} ion. For our discussion of the density of states, which is limited to an energy window of −7 to about 7 eV, we are primarily concerned with the Cr d, Mo d, and O p states, since the Sr-derived states appear at higher energy. The bands below −2 eV are predominantly of oxygen character. The presence of a cubic symmetry of the octahedral coordination of the oxygen atoms around the transition-metal Cr and Mo sites results in a splitting of the d levels of Cr and Mo sites into triply degenerate t_{2g} orbitals with lower energy and doubly degenerate e_g orbitals with higher energy. The Fermi level lies in the gap between the Cr $t_{2g_\uparrow}$ and Cr $e_{g_\uparrow}$ bands as shown in figure 2. The down-spin conduction band crossing E_F is dominated by the O 2p and Mo 4d t_{2g} states while the Cr 3d t_{2g} states have a smaller contribution. On the other hand, the up-spin band below E_F is mostly the Cr 3d t_{2g} and the O 2p states without any appreciable Mo 4d contribution; the sharp narrow up-spin band just above E_F is mostly of Mo t_{2g} and Cr e_g states. Summarizing our discussion we can state that the essential physical mechanism leading to ferromagnetism is very similar for the perfect Sr_2CrMoO_6 and the Sr_2FeMoO_6 compounds. These features are comparable with those recently reported [16].

3.2. The effect of oxygen vacancies or/and AS defects

For cases with imperfections, three situations were considered: (i) Sr_2CrMoO_6 with oxygen vacancies; (ii) Sr_2CrMoO_6 with antisite defects; (iii) Sr_2CrMoO_6 with oxygen vacancies and antisite defects. In the following we will discuss the oxygen vacancy or/and antisite imperfection effects on electronic structure and magnetic properties of Sr_2CrMoO_6 from the spin-polarized GGA + U method in detail.

3.2.1. Magnetic properties and electronic structure of Sr_2CrMoO_6 with oxygen vacancies. The effect of oxygen vacancies is simulated by taking away partial oxygen atoms from the supercell. We have studied particular cases having nearby two oxygen vacancies (figure 3). The inequivalent Cr and Mo sites are shown in figure 3. The calculated total magnetic moment and local magnetic moments are listed in table 2. Our calculations show that each local moment of Cr decreases by more than 0.2 μ_B except that the nearest neighbor μ_{Cr_8} (figure 3) of oxygen defects increases from 2.882 μ_B to 3.109 μ_B, and the absolute magnitude of all μ_{Mo} increases compared with that of perfect Sr_2CrMoO_6, especially for the nearest neighbor μ_{Mo_3} and μ_{Mo_4} of vacancies; the absolute magnitude increases from 0.636 μ_B to about 1.21 μ_B. The magnetic moments at each individual site decrease due to the different chemical environment induced by oxygen vacancies,

Table 2. The magnetic information of Sr_2CrMoO_6 with two oxygen vacancies and 25% AS with one/two oxygen vacancies, respectively. The first line gives the inequivalent Cr and Mo sites (figures 3, 6). The last two lines gives the magnetic information of 25% AS with one oxygen vacancy and 25% AS with two oxygen vacancies.

μ_{Cr_1}	μ_{Cr_2}	μ_{Cr_3}	μ_{Cr_4}	μ_{Cr_5}	μ_{Cr_6}	μ_{Cr_7}	μ_{Cr_8}	μ_{Mo_1}	μ_{Mo_2}	μ_{Mo_3}	μ_{Mo_4}	μ_{Mo_5}	μ_{Mo_6}	μ_{Mo_7}	μ_{Mo_8}	μ_T
2.616	2.632	2.617	2.617	2.617	2.617	2.565	3.109	−0.705	−0.658	−1.211	−1.214	−0.758	−0.760	−0.706	−0.659	1.750
−2.702	2.711	2.705	2.732	2.706	2.732	−2.938	3.076	−0.098	−0.200	−0.205	0.082	0.021	−0.139	−0.132	−0.129	1.250
−3.012	2.716	2.698	2.738	2.706	2.739	−3.012	3.132	−0.114	−0.160	−0.166	0.076	−0.163	−0.125	−0.173	−0.176	0.838

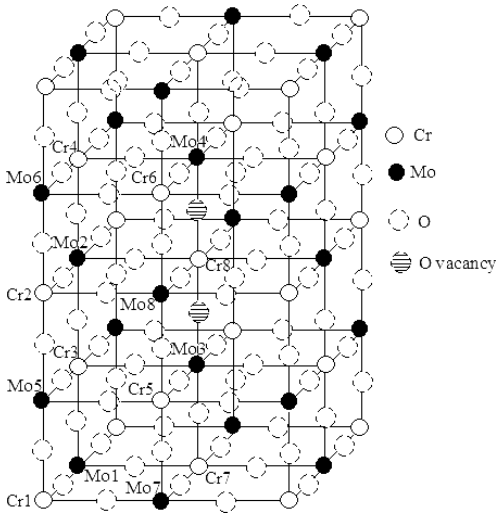

Figure 3. The lattice structures of Sr_2CrMoO_6 with two oxygen vacancies situated at an Mo–Cr–Mo bond in the z direction.

without any effect on the nature of the spin ordering. The μ_T only reduces by about 0.25 μ_B compared with the ordered case. The change of magnetic properties comes mainly from a variation of the local magnetic moments on the atoms directly concerned by the oxygen defects, i.e. the Cr and Mo atoms of the broken Cr–O–Mo bond. The segmental Cr–O–Mo bonds into the unit cell become Cr–Mo bonds. The coupling of Cr–O and Mo–O is reduced. Then, the antiferromagnetic coupling between Cr and Mo is enhanced. At the same time, we note that the local magnetic moments of Cr (Mo) atoms except the nearest neighbor Cr (Mo) atoms of oxygen vacancies are related to the distances between Cr (Mo) and oxygen defects. The greater the distances between Cr (Mo) and oxygen defects, the smaller the change of $\mu_{Cr}(\mu_{Mo})$ compared with the perfect case.

The total and partial density of states (DOS) from GGA + U method, displayed in figure 2, show clearly that the half-metallic character remains for Sr_2CrMoO_6 with two oxygen vacancies situated at an Mo–Cr–Mo bond in the z direction, while the gap $E_g = [-0.74, 0.20]$ eV in the spin-up channel is suppressed compared with the gap $E_g = [-1.05, 0.52]$ eV of perfect Sr_2CrMoO_6. The partial density of states (DOS) (figure 2) shows that the reduction of the gaps for the oxygen vacancies come mainly from a broadening of the occupied Cr $t_{2g_\uparrow}$ states and the unoccupied Mo $t_{2g_\uparrow}$ orbitals resulting from the change of crystal field around Cr and Mo atoms. For example, the crystal field of Cr_8 (figure 3) changes from oxygen octahedron to oxygen quadrangle, the triply degenerate t_{2g} and doubly degenerate e_g orbitals further split into d_{yz}, d_{xz}, d_{xy} and d_{z^2}, $d_{x^2-y^2}$ states and the d_{z^2} band moves upwards, whereas $d_{xy}(d_{x^2-y^2})$ orbitals move downwards, thus the bandwidth of Cr 3d bands below E_F is enhanced. The minority spin electronic structure is much affected by oxygen defects. The spin-down bandwidth is enhanced and the occupied Mo $t_{2g_\downarrow}$ increases while the unoccupied Mo $t_{2g_\downarrow}$ decreases associated with the broken Cr–O–Mo bonds.

3.2.2. Magnetic properties and electronic structure of Sr_2CrMoO_6 with AS defects. The effect of AS defects is simulated by interchanging the Cr and Mo sites, respectively, so as to generate different chemical environments surrounding each inequivalent Cr and Mo site while keeping the concentration of Cr/Mo fixed. We have performed the calculation for two different AS concentrations (25% and 50%), which are a little different from the experimental concentrations [15, 10]. Nevertheless, such calculations can provide useful information about the electronic and magnetic properties. The AS concentration is defined as the ratio of the concentration of B cations in B′ positions divided by the total concentration of B cations. The structures we have used are fully relaxed. Firstly, we examine the stability of solutions with parallel and anti-aligned magnetic moment on the Cr antisite into the cell. The calculations show that it is the most stable when Cr cations situated on Mo sites are antiparallel with the Cr cations of the regular sites. The total energy of the AP state (anti-aligned antisite) is more than 0.32 eV lower than the ground state, where all Cr moments are parallel. Then, we found the most favorable configuration (configuration A, 25%; configuration B, 50%) for the AS defects (figure 4) by calculating the ground energies of possible configurations. Configuration A is obtained by interchanging Cr_1 and Mo_4 sites at (0.0, 0.0, 0.0) and (0.5, 0.5, 0.5) positions, respectively. Configuration B is obtained by interchanging $Cr_1(Cr_3)$ and $Mo_1(Mo_4)$ at (0.0, 0.0, 0.0) ((0.5, 0.5, 0.5)) and (0.0, 0.0, 0.5) ((0.5, 0.5, 0.0)), respectively. The structure of configuration A is also cubic ($a = b = c = 7.872$ Å), while the structure of configuration B transforms into a tetragonal one ($a = b = 7.909$ Å, $c = 7.835$ Å). In the following we will only study the magnetic properties and electronic structure of the most favorable configurations.

Our calculated AS models yield the ground state to be magnetic with a reduced magnetic moment per formula unit (1.020 μ_B for the A configuration, 0.0 μ_B for the B configuration) compared to that of the fully ordered sample (2.0 μ_B). Simple considerations then show that an AS concentration around 37.5% is required to account for the experimental reduction of 1.5 μ_B/f.u. The calculated results

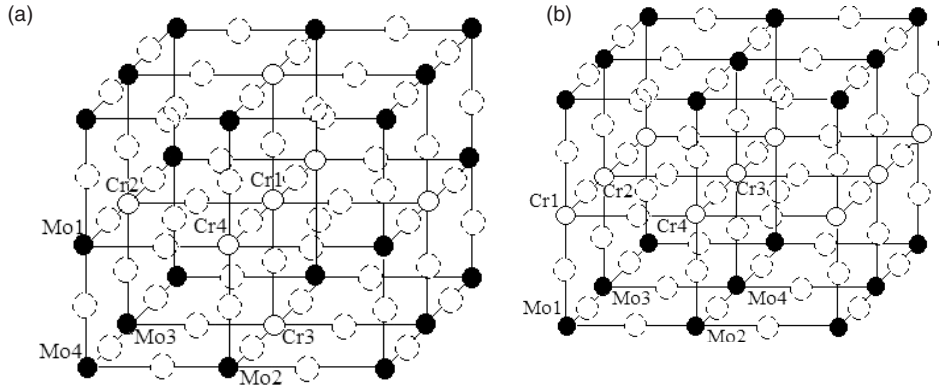

Figure 4. Representation of the disorder structures considered in this paper. (a) 25% ASs; (b) 50% ASs.

Table 3. Calculated magnetic information for Sr_2CrMoO_6 with antisite (AS) imperfections. The second column gives the inequivalent Cr and Mo sites shown in figure 4. The third column gives the number of Cr and/or Mo neighbors.

AS concentration	Sites	nn (next neighbour)	Magnetic moment (μ_B)	Net moment per f.u. (μ_B)
25%	Cr_1	6Cr	−2.736	1.020
(Config. A)	Cr_2	2Cr + 4Mo	2.707	
	Cr_3	2Cr + 4Mo	2.707	
	Cr_4	2Cr + 4Mo	2.707	
	Mo_1	4Cr + 2Mo	−0.216	
	Mo_2	4Cr + 2Mo	−0.216	
	Mo_3	4Cr + 2Mo	−0.218	
	Mo_4	6Mo	−0.398	
50%	Cr_1	4Cr + 2Mo	−2.689	0.0
(Config. B)	Cr_2	4Cr + 2Mo	2.689	
	Cr_3	4Cr + 2Mo	−2.688	
	Cr_4	4Cr + 2Mo	2.689	
	Mo_1	2Cr + 4Mo	0.021	
	Mo_2	2Cr + 4Mo	−0.012	
	Mo_3	2Cr + 4Mo	−0.021	
	Mo_4	2Cr + 4Mo	0.012	

are in agreement with the experimental observation [10, 15] of a lower magnetic moment resulting from AS defects. In order to understand the microscopic origin of this reduction in the magnetic moment, we discuss below our result in some detail.

The ground-state magnetic structure for the 25% concentration is found to be the ferrimagnetic state where the Cr spins are aligned ferromagnetically if the Cr are in the correct positions, and antiferromagnetically if the Cr ions occupy Mo sites because of the antisite defects (table 3). The magnetic structure for the 50% ASs is the antiferromagnetic state. The local magnetic moments of inequivalent Cr and Mo (labeled in figure 4) are shown in table 3. Compared with the ordered configuration in table 1, the absolute magnitude of all μ_{Mo} decreases. We note that a strong bonding–antibonding splitting of Mo t_{2g} states is caused by the hybridization between the AS defect and the host. As a result, the up-spin Mo t_{2g} states become partially occupied, and the absolute magnitude of the induced negative Mo moment is decreased; even the magnetic moments of Mo in AS defect sites change their signs at AS = 50%. Therefore, the mechanism of the ordered sample [16] relying on the strong antiferromagnetic coupling between the Cr and Mo sites become irrelevant near the antisite defects. After considering the AS defects, the magnetic moments of the regular Cr sites located in the nearest neighborhood to the defect Cr sites become strongly polarized by the antiferromagnetic super-exchange interaction with the defect states, i.e., the model suggests antiferromagnetically coupled Cr–O–Cr bonds, whenever two Cr ions form near-neighbor pairs. The antiferromagnetic interaction can be easily shown to be equivalent to a ferromagnetic one for the atoms in the Cr sublattice. Thus, super-exchange enhances the tendency toward a ferromagnetic order in the original Cr sublattice. This leads to the formation of the ferrimagnetically coupled Cr clusters. Therefore, the experimentally observed reduction of the magnetic moment [11, 13] mainly arises from an antiferromagnetic coupling of Cr–O–Cr bonds in a disordered sample.

In figure 5 we show the total DOS and the partial Cr 3d, Mo 4d and O 2p DOS for the different AS concentration. It is obvious that the half-metallic character is highly sensitive to AS defects. This is not extremely surprising because several Cr–O–Mo bonds are concerned by such defects. For example, for the antisite considered in the section (figure 4), several Cr–O–Mo bonds into the unit cell become X–O–X (X, Y = Cr or Mo), while two oxygen vacancies concern only one Mo–O–Cr–O–Mo bond and have consequently a more limited effect on the concerned atoms. Since the disorder has been introduced between Cr and Mo sublattices, the high lying Sr-derived states remain more or less unaffected. The bands below −2 eV are predominantly of oxygen character. Two sharp narrow bands above 2.0 eV appear in the spin-up channel and spin-down channel, respectively, which are antibonding Cr t_{2g} states. In the spin-up channel, disordering fills up the gap between crystal-field-split Cr t_{2g} and Cr e_g states observed in the ordered DOS; admixture states of Mo $t_{2g_\uparrow}$, Cr $t_{2g_\uparrow}$ and O $p_\uparrow$ cross the Fermi level; the bonding Cr $t_{2g_\uparrow}$ states span the energy from about −1.64 to −0.38 eV; the Cr $e_{2g_\uparrow}$ mostly appear above 0.5 eV. In the spin-down channel, a strong bonding–antibonding splitting of Cr 3d states is caused by the hybridization between the AS defect and the host. Then, the occupied Cr $t_{2g_\downarrow}$ states are enhanced and move upwards, and the Cr moments in AS defect sites change their signs; at the

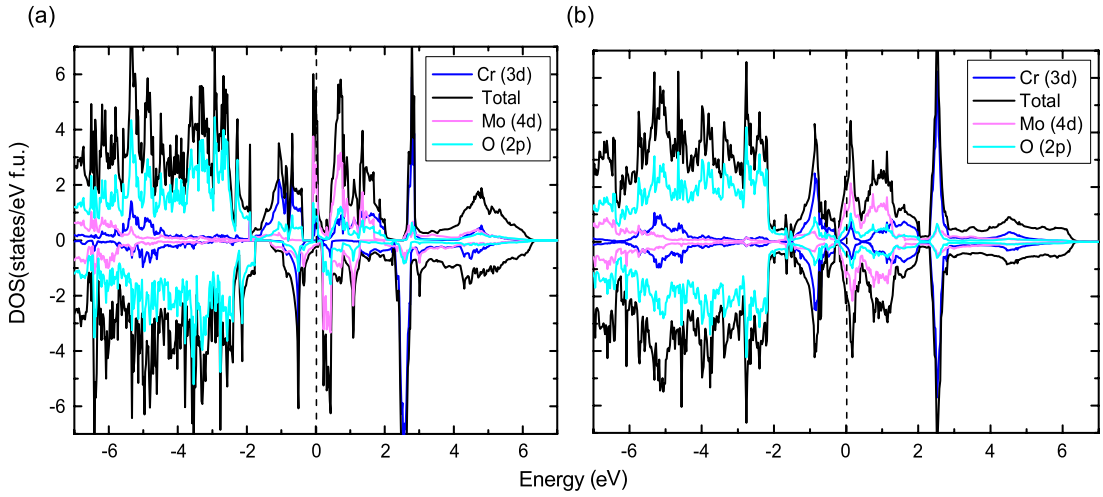

Figure 5. Total and partial densities of states of Sr_2CrMoO_6 with 25% and 50% ASs from GGA + U calculations. (a) 25% ASs, (b) 50% ASs. The spin-up and/or spin-down DOS is shown above and/or below the abscissa axis. The Fermi level is at zero energy.

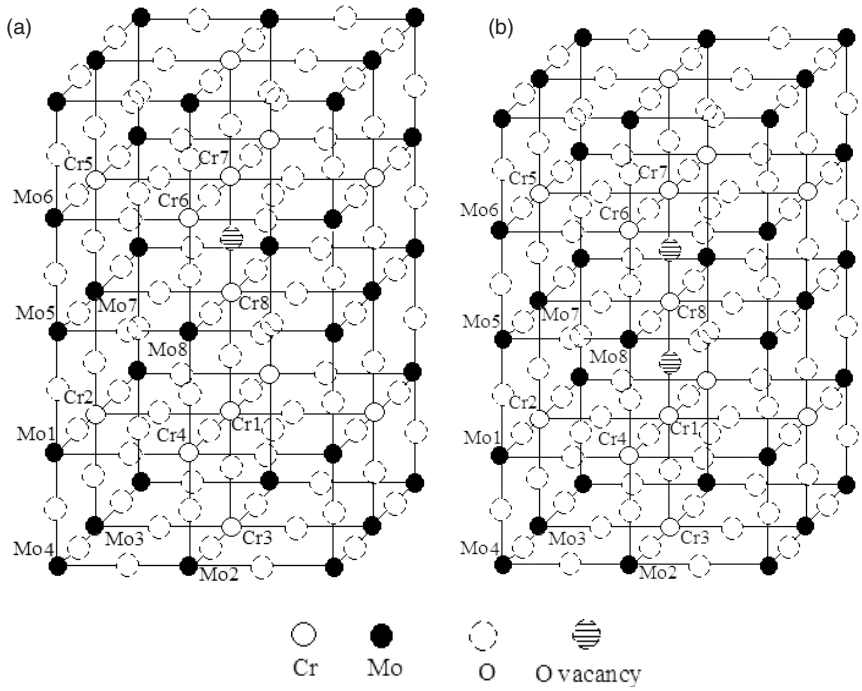

Figure 6. Representation of the disorder structures considered in this paper. (a) 25% ASs with one oxygen vacancy (b) 25% ASs with two oxygen vacancies.

same time, the antibonding Cr $t_{2g_\downarrow}$ states move downwards. It is important to note that there is only a moderate polarization of the states at and near E_F in 25% disordered configurations and nearly no polarization in 50% disordered configurations, in sharp contrast to the 100% polarization in the ordered sample.

3.2.3. Magnetic properties and electronic structure of Sr_2CrMoO_6 with oxygen vacancies and AS defects. Previously, the electronic band structure calculations indicated that the system shows metallic character when only AS defects are considered. In order to examine a possible semiconductor character resulting from a combination of oxygen vacancies and AS defects, we have studied particular cases having 25% ASs with one oxygen vacancy and two oxygen vacancies. Calculations are performed by constructing supercells with eight inequivalent Cr and eight inequivalent Mo positions. According to comparison of the ground energies of the possible configurations, the most favorable configurations are as shown in figure 6. The case can also be reasonably supposed because vacancies are well known to favor the atomic mobility inside compounds and it is reasonable to assume that a vacancy and an antisite form a pair of neighbors.

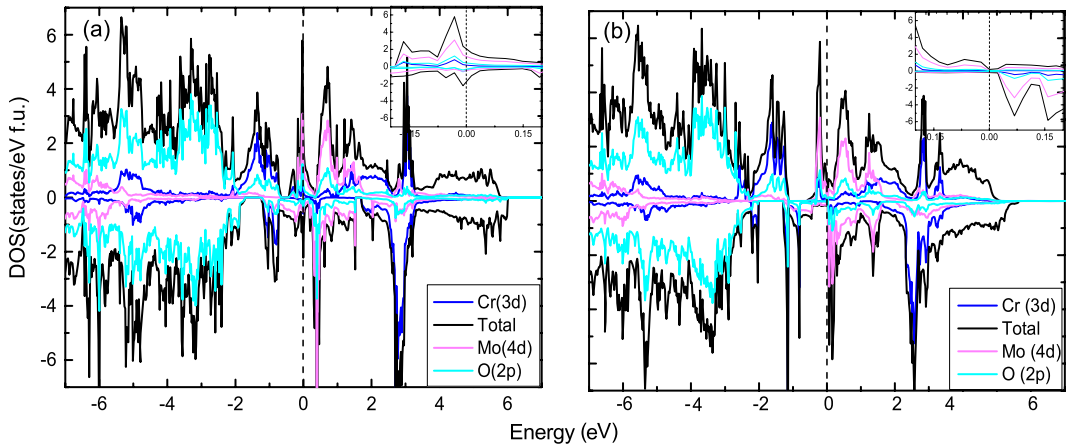

Figure 7. Total and partial densities of states of Sr_2CrMoO_6 with 25% ASs with one oxygen vacancy and two oxygen vacancies from GGA + U calculations. In the insets we present the total and partial densities of states around E_F. (a) 25% ASs and one oxygen vacancy; (b) 25% ASs and two oxygen vacancies. The spin-up and/or spin-down DOS is shown above and/or below the abscissa axis. The Fermi level is at zero energy.

The magnetic structure for the 25% concentration with oxygen vacancies is found to be the ferrimagnetic state where the spins are antiparallel between the Cr ions in the correct position and the Cr ions occupy Mo sites. Compared with the 25% AS disordered configuration in table 3, the local magnetic moment of Cr remains more or less the same except the atoms directly concerned by the oxygen defects, i.e. the Cr_7 (Cr_8) of figure 6(a) and the Cr_1 (Cr_7, Cr_8) of figure 6(b). It is visible that the absolute magnitude of local magnetic moments on the nearest neighbor Cr of the oxygen vacancy substantially increases. Because some Cr–O–Cr bonds of AS configuration into the unit cell become Cr–Cr bonds, the magnetic moments between the Cr in regular positions and the antisite Cr become direct antiferromagnetic super-exchange interactions. The mean magnitude of μ_{Cr} in the regular position increases. The increase may be explained by the strong antiferromagnetic (AFM) super-exchange interaction between the Cr at the correct sites and the Cr at the Mo sites, which enhances the ferromagnetism in the original Cr sublattice. Additionally, the magnetic moments of Cr (Mo) are also influenced by the distances between Cr (Mo) atoms and oxygen defects. The net magnetic moment of 25% ASs with one oxygen vacancy is enhanced by about 0.2 eV while the net magnetic moment of 25% ASs with two oxygen vacancies is reduced by about 0.2 eV compared to the 25% AS case. The difference may be caused by the competition between antiferromagnetic (AFM) super-exchange interaction and ferromagnetic interaction. Compared with the 25% AS sample, the increase of AFM interaction is larger than that of the ferromagnetic interaction.

Figure 7 shows the total DOS and the partial Cr 3d, Mo 4d and O 2p DOSs for the two disordered configurations; in the insets we present the total and partial densities of states around E_F. It is found that it is metallic for 25% ASs with one oxygen vacancy and there is only a moderate polarization, while for the case of 25% ASs with two oxygen vacancies there is a limited energy gap $E_g = 0.03$ eV. The calculated gap is smaller than the experimental value (0.1 eV). In view of the smaller values calculated by the VASP method, the band gap of the system would be larger in nature. Thus, it possibly has semiconducting behavior observed in experiment [11]. In the spin-up channel the bonding Cr t_{2g} shifts up relative to the AS case because the bonding–antibonding interaction increases resulting from the change of crystal field. Compared with the 25% AS configuration, the bonding Cr $t_{2g_\uparrow}$ states of 25% with one oxygen vacancy span the energy from −2.0 to −0.65 eV; the bonding Cr $t_{2g_\uparrow}$ states of 25% with two oxygen vacancies appear at energy approximately between −2.35 and −1.1 eV; the bonding Mo $t_{2g_\uparrow}$ slightly moves up by about 0.1 and 0.25 eV. In the spin-down channel the bonding Cr $t_{2g_\downarrow}$ states move upwards, especially for 25% ASs with two oxygen vacancies; the bonding Cr $t_{2g_\downarrow}$ states shift upwards by about 0.4 eV. A strong bonding–antibonding splitting of Mo t_{2g} states caused by the hybridization between the AS defect and the host, and the bonding Mo $t_{2g_\downarrow}$ states, slightly moves downwards for 25% ASs with one oxygen vacancy while the bonding Mo $t_{2g_\downarrow}$ states of 25% with two oxygen vacancies move upwards compared with AS defects for the difference of the crystal field. The limited gap of bonding–antibonding splitting just lies at E_F when 25% ASs with two oxygen vacancies is present. In the meantime we also simulate the system of 50% ASs with one or two oxygen vacancies. The electronic calculations show the system is still metallic.

It should be kept in mind that the supercell calculations are actually ordered calculations that make use of the translational symmetry, which is not the case of a truly disordered material. Furthermore, even though we have used reasonably large supercells, it is still a small number and therefore the various configurations that we can probe are limited.

4. Conclusions

We have performed electronic structure calculations for ordered and disordered Sr_2CrMoO_6. The effect of disorder has been modeled by supercell calculations. Our results reveal that the perfect Sr_2CrMoO_6 is half-metallic material;

the half-metallic feature is easily lost in the presence of imperfections; only oxygen vacancies can preserve this feature; it is metallic when 25% antisite concentration with or without one oxygen vacancy and 50% antisite concentration with or without oxygen vacancies are present, while the material is probably nonmetallic with the energy gap of 0.03 eV when 25% ASs with two oxygen vacancies are considered. We have shown that for AS defects the solutions of the AP states are the most stable whatever the nature of the imperfection is (with or without oxygen vacancies). The reduction in the magnetic moment is caused by the antiferromagnetic coupling between the Cr cations situated on Mo sites and the Cr cations of the regular sites. In order to account for the experimental reduction of 1.5 μ_B/f.u., an AS concentration around 37.5% is required. We have also shown that when only considering the AS defects the material is metallic; consequently, AS defects with oxygen vacancies could be an alternative explanation of the observed reduced magnetization.

Acknowledgment

The numerical calculation was carried out using the facilities of the Department of Physics in Nanjing Normal University.

References

[1] Jung A, Ksenofontov V, Reiman S, Therese H A, Kolb U, Felser C and Tremel W 2006 *Phys. Rev.* B **73** 144414
[2] Solovyev I V 2002 *Phys. Rev.* B **65** 144446
[3] Fisher B, Chashka K B, Patlagan L and Reisner G M 2004 *Phys. Rev.* B **70** 205109
[4] Kato H, Okuda T, Okimoto Y and Tomioka Y 2004 *Phys. Rev.* B **69** 184412
[5] Vaitheeswarana G, Kanchana V and Delin A 2005 *Appl. Phys. Lett.* **86** 032513
[6] Sleight A W and Ward R 1961 *J. Am. Chem. Soc.* **83** 1088
[7] Anderson M T, Greenwood K B, Taylor G A and Poeppelmeier K R 1993 *Prog. Solid State Chem.* **22** 197
[8] Galasso F S 1969 *Structure, Properties and Preparation of Perovskite-type Compounds* (London: Pergamon)
[9] Patterson F K, Moeller C W and Ward R 1963 *Inorg. Chem.* **2** 196
[10] Chana T S *et al* 2004 *Solid State Commun.* **131** 531–5
[11] Moritomo Y, Xu Sh, Machida A, Akimoto T, Nishibori E, Takata M and Sakata M 2000 *Phys. Rev.* B **61** R7827
[12] Blasco J *et al* 2002 *Solid State Sci.* **4** 651
[13] Arulraj A, Ramesha K, Gopalakrishnan J and Rao C N R 2000 *J. Solid State Chem.* **155** 233
[14] Shannon R D 1976 *Acta Crystallogr.* A **32** 751
[15] Arulraj A, Ramesha K, Gopalakrishnan J and Rao C N R 2000 *J. Solid State Chem.* **155** 233–7
[16] Bonilla C M, Landínez Téllez D A, Arbey Rodríguez J, Vera López E and Roa-Rojas J 2007 *Physica* B **398** 208–11
[17] Wu H 2001 *Phys. Rev.* B **64** 125126
[18] Blöchl P E 1994 *Phys. Rev.* B **50** 17953
[19] Kresse G and Joubert D 1999 *Phys. Rev.* B **59** 1758
[20] Kresse G and Furthmuller J 1996 *Phys. Rev.* B **54** 11169
[21] Kresse G and Furthmuller J 1996 *Comput. Mater. Sci.* **6** 15
[22] Anisimov V I, Zaanen J and Andersen O K 1991 *Phys. Rev.* B **44** 943
[23] Rohrbach A, Hafner J and Kresse G 2003 *J. Phys.: Condens. Matter* **15** 979
[24] Liechtenstein A I, Anisimov V I and Zaanen J 1995 *Phys. Rev.* B **52** R5467
[25] Dudarev S L, Botton G A, Savrasov S Y, Humphreys C J and Sutton A P 1998 *Phys. Rev.* B **57** 1505
[26] Solovyev I V, Dederichs P H and Anisimov V I 1994 *Phys. Rev.* B **50** 16861
[27] Korotin M A, Anisimov V I, Khomskii D I and Sawatzky G A 1998 *Phys. Rev. Lett.* **80** 4305
[28] Gross R *et al* 2000 *Proc. SPIE* **4058** 278